J Mater Sci: Mater Med (2011) 22:1431–1438
DOI 10.1007/s10856-011-4314-7

Spectral study of interaction between poly(L-lysine)–poly(ethylene glycol)–poly(L-lysine) and nucleic acids

Yu He · Qiujun Yan · Gongwu Song · Juan Chen

Received: 3 September 2010 / Accepted: 3 April 2011 / Published online: 23 April 2011

Abstract Polymer-DNA interactions have attracted considerable interests due to their important application in DNA transfection and cellular drug delivery technologies. In this work, a new detection assay for DNA is proposed with a tri-block copolymer poly(L-lysine)–poly(ethylene glycol)–poly(L-lysine) by resonance light scattering technique with the linear ranges from 0.0656 to 6.56 μg ml^{-1}. The detection limit for DNA is 0.42 ng ml^{-1}. Most coexisting substances do not interfere in the detection. UV-spectra and FTIR-spectra were employed to demonstrate the mechanisms of the interaction that the conformation of the DNA changes because the microenvironment of DNA changes.

1 Introduction

Non-viral gene delivery systems could improve safety and overcome tissue-tropism limitations associated with viral based gene therapies [1]. As two major classes of non-viral gene delivery system, cationic liposomes and polycations are widely investigated. Many different cationic lipids have been used for gene therapies [2–4]. Compared with other non-viral systems, complexes of polycations with DNA have advantages in the control of size and charge, and the hydrophilic–lipophilic characteristics of the transfecting species. To improve the stability of the polyplexes in aqueous solution and prevent their interactions with serum proteins, cationic block and graft copolymers were developed, which contain segments from polycations and nonionic water-soluble polymers [5–8]. Graft copolymers have a comb-like structure with hydrophilic segments attached on the side of the cationic segments. There are some reports about coating the polyion complex of a polycation and DNA with a hydrophilic polymer to form micelle-like associates using graft copolymers [8, 9]. Block copolymers composed of a cationic segment and a hydrophilic segment spontaneously associate with polyanionic DNA to form block copolymer micelles. The distinct feature of the associate is that the core of the polyion complex between DNA and the polycation is coated by a layer of the hydrophilic polymer, which endows the associate with a high colloidal stability and reduced interaction with blood components. These desirable properties are the major advantages of the micellar DNA delivery system for in vivo application [10]. Block copolymer micelles entrapping plasmid DNA and oligonucleotides have been developed as non-viral DNA delivery systems [11–13].

In 1993, Pasternack firstly used resonance light scattering (RLS) technique to investigate an assembly phenomenon of dyes on nucleic acids [14]. This technique is generally coupled to other spectral analysis techniques such as absorption, fluorescence and CD, and can compensate for the drawbacks of spectrophotometric and spectrofluorometric measurements [15]. Being a novel and promising analytical technique, with high sensitivity and easy operation, it was utilized in the detection of bimolecular, and extending the usefulness of reagents in the quantitative analysis of medicines, proteins and nucleic acids with various probes [16–18]. In recent years, it has been widely applied to determine the amount of DNA in samples with various light scattering probes, such as polymers [19, 20], organic dyes [21, 22], surfactants [23, 24], metal ion and metal complex [25–27].

Y. He · Q. Yan · G. Song (✉) · J. Chen
Ministry-of-Education Key Laboratory for the Synthesis and Application of Organic Function Molecules, Hubei University, Wuhan 430062, People's Republic of China
e-mail: songgw@hubu.edu.cn

Herein, a new detection assay for DNA is proposed with a tri-block copolymer poly(L-lysine)–poly(ethylene glycol)–poly(L-lysine) (PLL–PEG–PLL) by RLS technique. Most coexisting substances do not interfere in the detection. UV-spectra and FTIR-spectra were employed to demonstrate the mechanisms of the interaction that the conformation of the DNA changes because the microenvironment of DNA changes. It is also proved that the tri-block copolymer can be used as non-viral gene delivery systems [28]. The present paper investigates the interaction of PLL–PEG–PLL with DNA using RLS, IR, and UV-spectroscopy, which are helpful to clarify the mechanism of the tri-block copolymer effects on the structure and physical properties of DNA.

2 Experimental section

2.1 Apparatus

The RLS spectra were measured with a Shimadzu RF-540 spectrofluorometer with a 1 × 1 cm cross-section quartz cell (Tokyo, Japan). The FTIR-spectra of PLL–PEG–PLL–DNA complex were obtained on Perkin-Elmer Spectrum One after the complex was dried at 40°C under vacuum, the solid calf thymus DNA (ctDNA) and PLL–PEG–PLL were used directly to obtain FT-IR spectrum. The UV absorption measurements were performed on a Perkin-Elmer λ-17 UV/VIS spectrophotometer (PE Co., America). A WH-2 vortex mixer (Huxi Instrumental Co., Shanghai, China) was used to blend the solution, and a pHB-4 pH meter was used to measure the pH of the solution.

2.2 Reagents

Poly(L-lysine)–poly(ethylene glycol)–poly(L-lysine) was synthesized by our coworkers as reference [29]. The working concentration of PLL–PEG–PLL solution was 8.32×10^{-3} mol l^{-1}. Complete DNA (Baitai Biochemical Co., Chinese Academy of Sciences) dissolution was achieved over a period of 24 h or longer under occasional shaking of the suspension. The concentrations of stock solutions of nucleic acids were determined by the absorbance at 260.0 nm. The working concentration of the nucleic acid, which is prepared by diluting the stock solution with double-distilled water, was 2.6×10^{-4} mol l^{-1}. Pyrene (Py) (Alfa Aesar) was dissolved in methanol and the prepared concentration was 1.285×10^{-3} mol l^{-1}. Tris (hydroxymethyl) aminomethane–HCl (Tris–HCl) solution was used to control the acidity. 0.1 mol l^{-1} NaCl was used to adjust the ionic strength of the aqueous solutions. Double-distilled water is used throughout the work.

2.3 Methods

Appropriate volumes of PLL–PEG–PLL and DNA solution were added into a dry 25 ml volumetric flask, and then diluted to 12.5 ml with double-distilled water and vortexes to form the solutions of (PLL–PEG–PLL)–DNA complex. After 5 min, the light scattering spectrum was obtained by scanning simultaneously with the same excitation and emission wavelengths. The RLS intensity was measured with both the excitation and emission wavelengths at 360 nm and slits at 10 nm. All the RLS spectra and the UV absorption spectra were obtained against the corresponding spectrum of the blank which was treated in the same procedure.

3 Results and discussion

3.1 RLS spectra

Resonance light scattering is a valuable technique for quantification of DNA since the enhanced RLS signals can be easily measured by using a common spectrofluorometer for aggregated species or large particles in nanometer scale near UV absorption bands. Figure 1 displayed the RLS spectra of (PLL–PEG–PLL)–DNA system. The RLS intensity of PLL–PEG–PLL was rather weak in the wavelength range of 200–700 nm. However, after adding of DNA, the RLS intensity was strongly enhanced and reached the maximum at 363 nm. The RLS intensity increased as the concentration of DNA increased. This phenomenon indicates a strong interaction between PLL–PEG–PLL and DNA since PLL–PEG–PLL could be easily combined with polyanion of DNA through electrostatic attractions to form aggregates. Thus DNA could be detected based on this method.

3.2 Effect of ratio of PLL–PEG–PLL to DNA

Figure 2 exhibited the RLS intensity depended on the ratios of PLL–PEG–PLL to DNA based on the molar ratios of N atoms of PLL–PEG–PLL and P atoms of DNA. DNA was mixed with PLL–PEG–PLL by single-step addition at N:P ratios of 0–2.0. The RLS intensity increased as the ratios varied from 0 to 2.0, with particularly steeply rise between ratios 0.8–1.0 when the concentrations of DNA were from 2.08×10^{-5} to 4.16×10^{-6} mol l^{-1}. Above ratio 1.0 there was little further increase of the RLS intensity. These data suggested few changes in DNA morphology at low N:P values, with self-assembly of discrete nanoparticles occurring between 0.8 and 1.0. It can be deduced that 1:1 complex was formed.

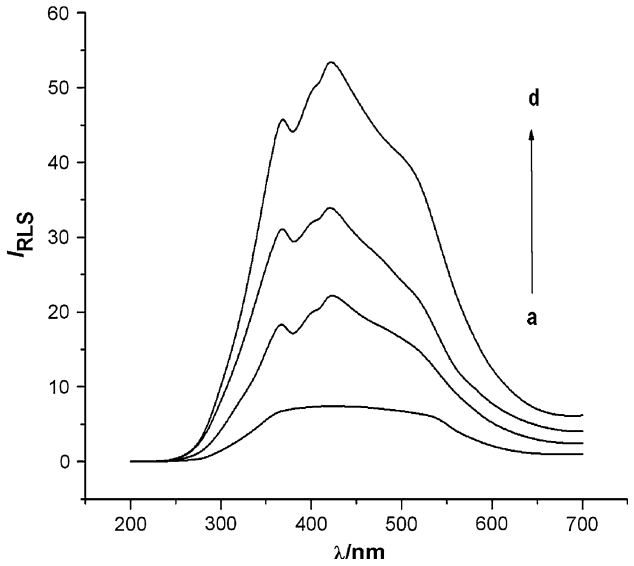

Fig. 1 The resonance light scattering spectra of (PLL–PEG–PLL)–DNA system. *a* 6.66×10^{-5} mol l^{-1} PLL–PEG–PLL; *b–d* the mixture of 6.66×10^{-5} mol l^{-1} PLL–PEG–PLL with 1.4×10^{-5}, 2.8×10^{-5} and 4.2×10^{-5} mol l^{-1} DNA

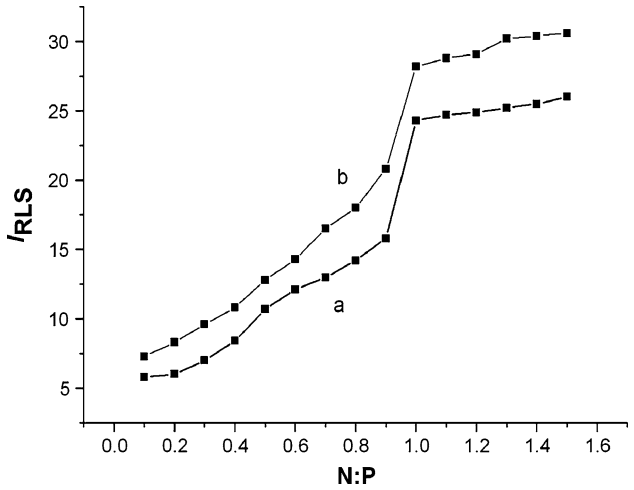

Fig. 2 The effect of the N:P ratio on the RLS intensity of (PLL–PEG–PLL)–DNA system with different concentrations of DNA. The concentration of DNA: *a* 2.08×10^{-5} mol l^{-1}; *b* 4.16×10^{-6} mol l^{-1}

3.3 Effect of pH

Figure 3 illustrated the RLS spectra of (PLL–PEG–PLL)–DNA, PLL–PEG–PLL, and DNA when the pH value was ranging from 1.5 to 10. The RLS intensity of PLL–PEG–PLL had no variation within the experimental pH range while the RLS intensity of DNA increased as decreasing pH value at pH < 3.0 due to the nitrogen atoms of DNA binding H^+ ions under strongly acidic condition, causing some aggregates in the size 200–700 nm [18–20]. The RLS

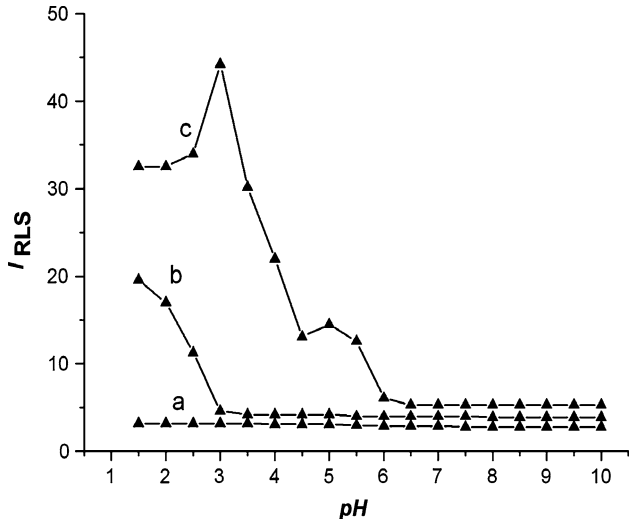

Fig. 3 The effect of pH on the (PLL–PEG–PLL)–DNA system. *a* 8.32×10^{-6} mol l^{-1} PLL–PEG–PLL; *b* 8.32×10^{-6} mol l^{-1} DNA; *c* 8.32×10^{-6} mol l^{-1} PLL–PEG–PLL and 8.32×10^{-6} mol l^{-1} DNA

intensity of the (PLL–PEG–PLL)–DNA system was dependent on the pH value, and reached the maximum at pH 5.0. The interaction between DNA and PLL–PEG–PLL was through the positively charged amine group of PLL–PEG–PLL with the negatively charged phosphate of DNA. The states of the DNA and PLL–PEG–PLL were affected by the pH value, so were the total charge of the DNA and PLL–PEG–PLL, which may affect the formation of the complex. Thus the RLS intensity changed with the changing of pH value. So the optimum pH for the (PLL–PEG–PLL)–DNA system was 5.0.

3.4 Effect of ionic strength

The ionic strength of the system was controlled by 0.1 mol l^{-1} NaCl solution and Fig. 4 presented the ionic strength effected on the formation of the (PLL–PEG–PLL)–DNA complex. The results indicated that the RLS intensity of the system enhanced rapidly when the ionic strength under 4.8×10^{-3} mol l^{-1}. And then the RLS intensity of the system decreased and kept no change when the ionic strength further increased. The cause may be that the ionic strength had at some extent impact on electronic interaction between PLL–PEG–PLL and DNA, the cooperative binding of the complex bosomed weaker and the dissociation of the complex occurred [29]. The RLS intensity of PLL–PEG–PLL did not have any variation with ionic strength.

3.5 Incubation time and the stability of the system

The influence of incubation time on the RLS intensity enhanced by DNA was investigated immediately after

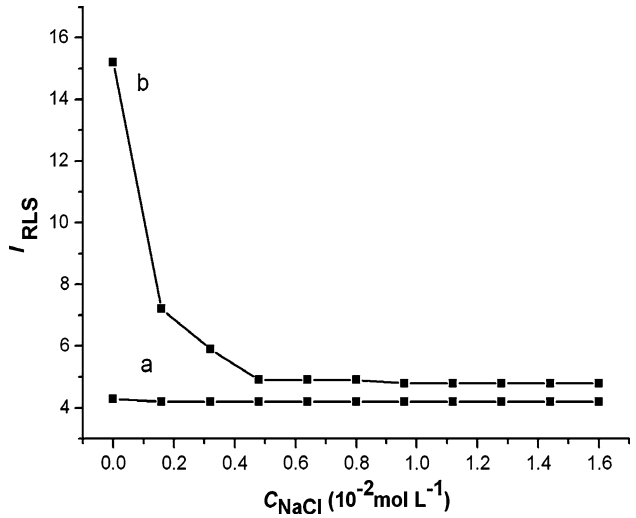

Fig. 4 The effect of ionic strength on the (PLL–PEG–PLL)–DNA system. *a* 8.32×10^{-6} mol l^{-1} PLL–PEG–PLL; *b* 8.32×10^{-6} mol l^{-1} PLL–PEG–PLL and 8.32×10^{-6} mol l^{-1}

Table 1 The effect of incubation time on the PLL–PEG–PLL enhanced by DNA

Time (min)	0	10	20	30	40	60	80	100	120
I_{RLS}	19	19	19	19	19.1	18.6	18.6	18.7	18.8

$C_{PLL–PEG–PLL}$: 8.32×10^{-6} mol l^{-1}; C_{DNA}: 8.32×10^{-6} mol l^{-1}

mixing PLL–PEG–PLL and DNA in pH 5.0 buffer solution, as summarized in Table 1. The data showed a nearly constant RLS intensity, indicating that the stable scattering signal for the determination of DNA.

3.6 Selectivity of this method

The influence of co-existing species, such as metal ions, BSA, and Glucose on the RLS intensity of the complex was summarized in Table 2. It can be seen that most of the substances tested did not interfere on the determination of DNA.

3.7 Calibration curve

The calibration curve was obtained according to the above standard procedure. As shown in Fig. 5, there existed a linear relationship between the RLS intensity and the concentration of DNA within the range of 0.0656–6.56 μg ml^{-1}. The linear regression equation was $I = 7.796 + 3.343\ C_{(DNA)}$, $r = 0.9987$. The detection limit (3σ) was 0.42 ng ml^{-1}.

3.8 Analysis

In the optimum conditions, three synthesis samples including some foreign species were prepared. As shown in Table 3, the determination of DNA using PLL–PEG–PLL as the probe via RLS technique was sensitive and reproducible.

Table 2 The interferences of foreign substances

Foreign substances	Concentration (mg l^{-1})	$\Delta I_{RLS}/I_{RLS}$ (%)
Ba^{2+}	0.00256	−0.53
Zn^{2+}	0.00256	+1.01
Br^{-}	0.0256	+1.06
Cr^{3+}	0.000064	+2.13
Fe^{3+}	0.0064	+2.66
Cu^{2+}	0.00032	−2.13
BSA	0.000032	+6.38
Gly	0.16	+5.31
L-cysteine	0.000384	+5.31
Glucose	0.001966	+2.13
As^{5+}	0.08	−3.72
K^{+}	0.00064	+1.06
Mn^{2+}	0.16	+5.85
Sn^{4+}	0.08	+5.32
Pb^{2+}	0.016	−4.20
Ni^{2+}	0.016	+2.66
Hg^{2+}	0.04	−3.72

$C_{PLL–PEG–PLL}$: 8.32×10^{-6} mol l^{-1}; C_{DNA}: 8.32×10^{-6} mol l^{-1}

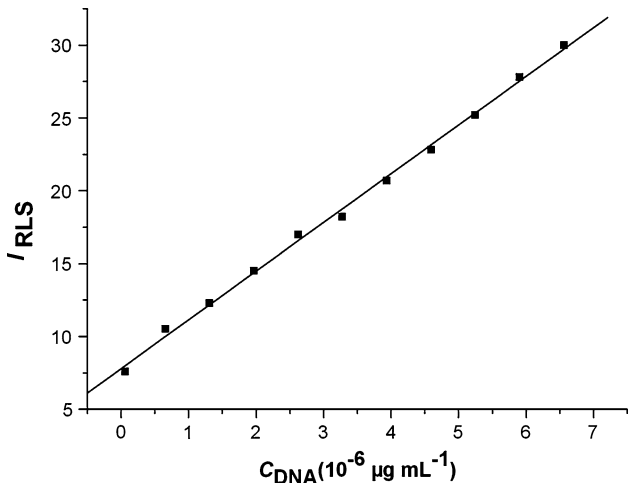

Fig. 5 Calibration curve. The concentration of PLL–PEG–PLL: 4.16×10^{-6} mol l^{-1}

3.9 The mechanism of the interaction

Figure 6 displayed the absorption spectra of the PLL–PEG–PLL–DNA system. It was showed that the absorbance of DNA at 260 nm increased when the concentration of the PLL–PEG–PLL increased. The absorbance at $\lambda > 320$ nm increased with the increase of the concentration of the PLL–PEG–PLL resulted from the formation of

Table 3 Determination result of synthetic sample

Sample	Concentration of DNA (mg ml^{-1})	Foreign substances[a]	Found (mg ml^{-1})	Recovery (%)	R.S.D.[b] (%)
ctDNA	0.20	Cr^{3+}, Br^{-}, K^{+}	0.21	105	1.95
ctDNA	0.50	Pb^{2+}, Sn^{4+}, Mn^{2+}	0.51	102	1.72
ctDNA	0.80	Zn^{2+}, Ba^{2+}, Cu^{2+}	0.78	97.5	2.57

[a] $C_{Cr^{3+}} = 0.02$ mg l^{-1}; $C_{Br^{-}} = 20$ mg l^{-1}; $C_{K^{+}} = 10$ mg l^{-1}; $C_{Zn^{2+}} = 10$ mg l^{-1}; $C_{Ba^{2+}} = 10$ mg l^{-1}; $C_{Cu^{2+}} = 0.05$ mg l^{-1}; $C_{Pb^{2+}} = 0.1$ mg l^{-1}; $C_{Sn^{4+}} = 1$ μg l^{-1}; $C_{Mn^{2+}} = 5$ mg l^{-1}

[b] $n = 5$

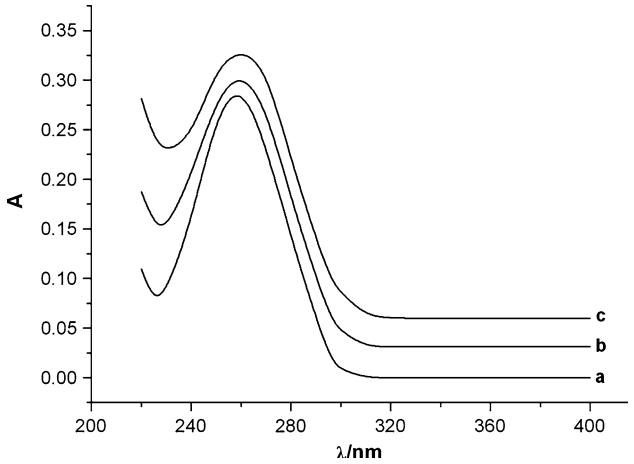

Fig. 6 UV spectra of (PLL–PEG–PLL)–DNA system. C_{DNA}: 5.1×10^{-5} mol l^{-1}. $C_{PLL-PEG-PLL}$: *a* 1.63×10^{-5} mol l^{-}; *b* 4.88×10^{-5} mol l^{-1}; *c* 8.15×10^{-5} mol l^{-1}

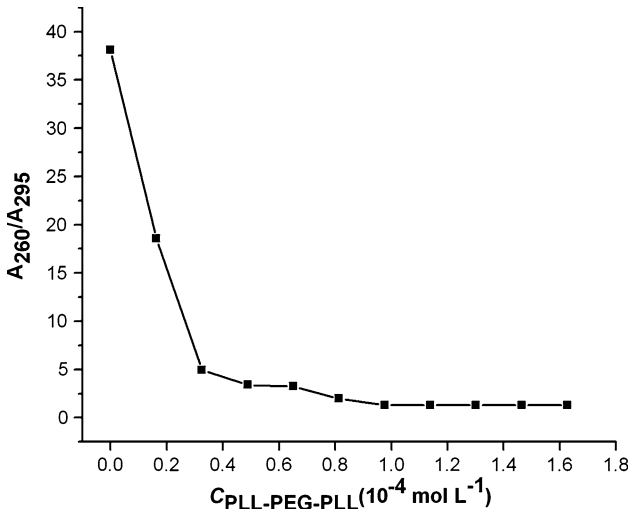

Fig. 7 Effect of the concentration of PLL–PEG–PLL on the A_{260}/A_{295}. C_{DNA}: 5.1×10^{-5} mol l^{-1}

compact light scattering particles [30]. Figure 7 demonstrated the effect of concentration of PLL–PEG–PLL on the A_{260}/A_{295}. It presented that the ratio decreased sharply with the increase of the concentration of PLL–PEG–PLL, which indicated a specific influence of PLL–PEG–PLL on DNA secondary structure. It was reported that A_{260}/A_{295} decreases with the transition of the conformation from B-type to Z-type of poly(dG-dC) · (dG-dC) in the presence of high salt concentration of polyamine [31]. Therefore, DNA could turn from B-type to Z-type when the concentration of PLL–PEG–PLL reached certain range.

Figure 8 displayed the FTIR-spectra of (PLL–PEG–PLL)–DNA complex, DNA, and PLL–PEG–PLL. The main absorption band of DNA were observed at: 1091 cm^{-1}, corresponding to the symmetric stretching vibration of phosphate groups; 1238 cm^{-1}, the anti symmetric stretching vibration of phosphate group; 1003 cm^{-1}, the vibration of C=N of ribose; 1640 cm^{-1}, the vibrations of C_6=O of guanine and C_4=O of thymine. Compare to Microscopic FTIR-spectra of DNA, there was some shift [32]. Apparently the main characteristic absorption bands of the DNA shifted from 1091, 1238 and 1640 cm^{-1} to 1088, 1230, and 1643 cm^{-1}, respectively, confirming the interaction between PLL–PEG–PLL and DNA had happened. Also the shapes of the absorption had changed, which was another evidence of the interaction. The absorption band at 1003 cm^{-1} was the characteristic of B-conformation DNA. The disappearance of it in absorption band of the (PLL–PEG–PLL)–DNA complex was the evidence that the interaction has altered the B-conformation of DNA.

Figure 9 shows the emission spectra of pyrene with and without PLL–PEG–PLL to study the aggregation behavior of polymer. The low solubility of pyrene in water results in the low fluorescence intensity of pyrene. However, the solubility increases significantly in hydrophobic environment, which leads to the increase of fluorescence intensity [33]. In Fig. 9, enhanced fluorescence intensities with slight red shifts for the five peaks of pyrene are observed when the concentration of PLL–PEG–PLL increases, which indicates the formation of hydrophobic micro-domain. With the rising concentration, PLL–PEG–PLL molecules transform from monomer states to micelles via aggregation. Then the hydrophobic pyrene probe will move from aqueous solution to the hydrophobic micro-domain of PLL–PEG–PLL micelles [34].

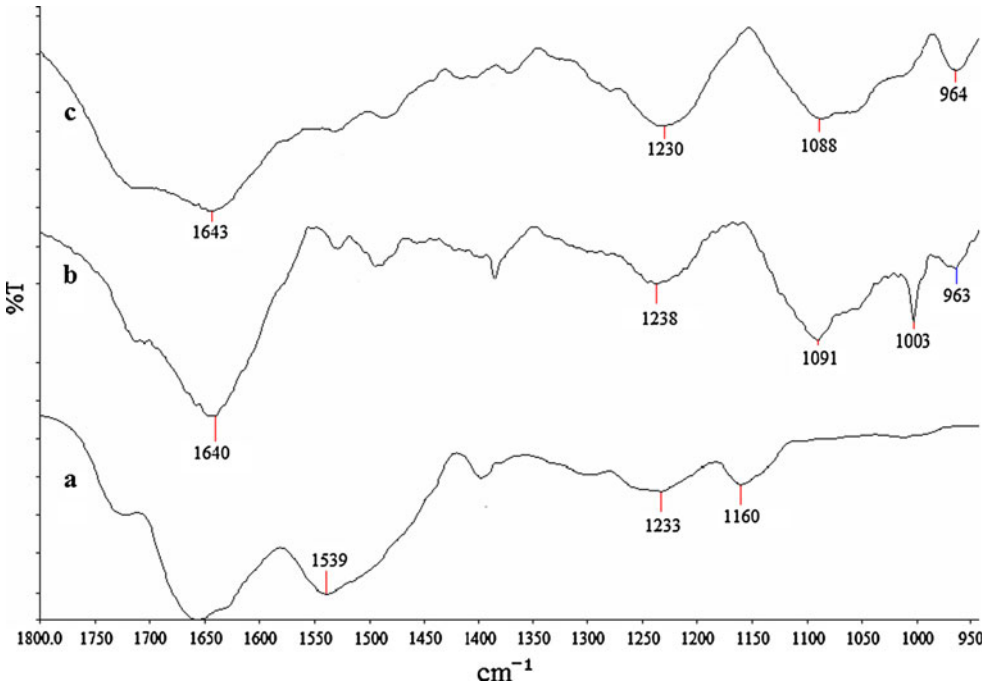

Fig. 8 FTIR-spectra of the (PLL–PEG–PLL)–DNA system. *a* PLL-PEG-PLL; *b* DNA; *c* (PLL–PEG–PLL)–DNA

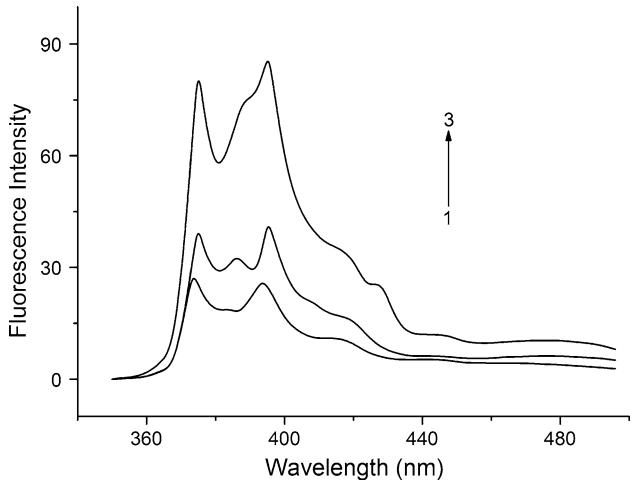

Fig. 9 Fluorescence emission spectra of pyrene probe in the presence of PLL–PEG–PLL. $1 \rightarrow 3$: $C_{pyrene} = 1.285 \times 10^{-6}$ mol^{-1}; $C_{PLL-PEG-PLL}$ (mol l^{-1}): 0, 6×10^{-4}, 7.5×10^{-4}

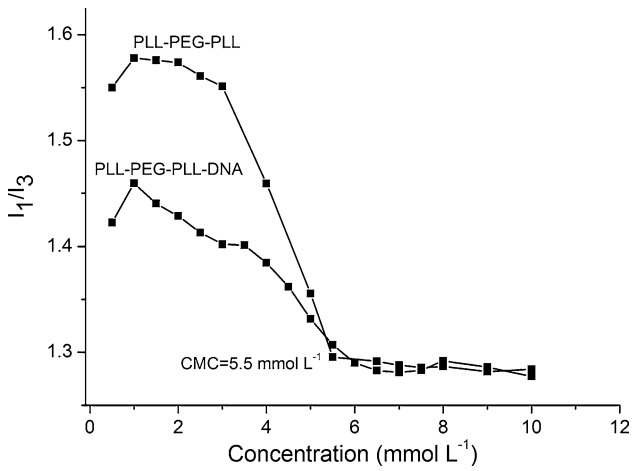

Fig. 10 Dependence of I_1/I_3 on PLL–PEG–PLL concentration with and without DNA. $C_{pyrene} = 1.285 \times 10^{-6}$ mol l^{-1}; $C_{DNA} = 5.1 \times 10^{-5}$ mol l^{-1}

Figure 10 is the plot of I_1/I_3 against PLL–PEG–PLL concentration with and without DNA to determine the interaction of PLL–PEG–PLL with DNA and calculate its cmc. In the absence of DNA, I_1/I_3 doesn't change greatly at low PLL–PEG–PLL concentration, which implies that nearly no hydrophobic micro-domain was formed in the solution [33, 34]. A sudden sharp decrease in I_1/I_3 occurs later, which reflects the decreasing polarity of the microenvironment and the pre-micellar formation. When further PLL–PEG–PLL concentration increases, I_1/I_3 reaches a platform because the surfactant molecule in the pre-micelle increases and then real micelle forms. As displayed in Fig. 10, the cmc value for PLL–PEG–PLL is about 5.5 mmol/l. The phenomena confirm the process that pyrene probe gradually transfers from water into the core of pre-micelles and at last micelles.

For DNA–PLL–PEG–PLL system, in the presence of DNA, I_1/I_3 displays similar changes. However, when PLL–PEG–PLL concentration is lower than CMC, the I_1/I_3 values and the D value of I_1/I_3 decline (from 1.58 to 1.28) are much lower than those of pure PLL–PEG–PLL solutions (from 1.46 to 1.28), which reveals the micro-environmental polarity of DNA/PLL–PEG–PLL complex was lower than that of free PLL–PEG–PLL micelle solution and the cooperative association reaction between DNA and PLL–PEG–PLL was weaker than that among PLL–PEG–PLL molecules [35].

4 Conclusion

The PLL–PEG–PLL was employed as a new probe to detect DNA via RLS method, which is sensitive, convenient, reproducible and rapid. The maximum RLS intensity was observed when 1:1 complex of (PLL–PEG–PLL)–DNA was formed. The foreign species have no impact on the RLS signal of the system. The mechanism of the tri-block copolymer effects on the structure and physical properties of DNA was also demonstrated. It is also proved that the tri-block copolymer was potential as non-viral gene delivery systems.

Acknowledgments This work was financially supported by the Scientific Research Foundation of Education Commission of Hubei Province (Q201101 and Q20111010).

References

1. Feng L, Leaf H. Development of non-viral vectors for systemic gene delivery. J Control Release. 2002;78:259–66.
2. Chu Q, Tousignant JD, Fang S, Jiang C, Eastman SJ, Chen LH, Cheng SH, Scheule RK. Binding and uptake of cationic lipid: pDNA complexes by polarized airway epithelial cells. Hum Gene Ther. 1999;10:25–36.
3. Blezinger P, Freimark BD, Matar M, Wilson E, Singhal A, Min W, Nordstrom JL, Pericle F. Intratracheal administration of interleukin 12 plasmid-cationic lipid complexes inhibits murine lung metastases. Hum Gene Ther. 1999;10:723–31.
4. Kaneda Y, Saeki Y, Nakabayashi M, Zhou WZ, Kaneda MW, Morishita R. Enhancement of transgene expression by cotransfection of oriP plasmid with EBNA-1 expression vector. Hum Gene Ther. 2000;11:471–9.
5. Kabanov AV, Vinogradov SV, Suzdaltseva YG, Alakhov VYu. Water-soluble block polycations as carriers for oligonucleotide delivery. Bioconjug Chem. 1995;6:639–43.
6. Kataoka K, Togawa H, Harada A, Yasugi K, Matsumoto T, Katoyose S. Spontaneous formation of polyion complex micelles with narrow distribution from antisense oligonucleotide and cationic block copolymer in physiological saline. Macromolecules. 1996;29:8556–7.
7. Choi YH, Liu F, Choi JS, Kim SW, Park JS. Characterization of a targeted gene carrier, lactose-polyethylene glycol-grafted poly-L-lysine, and its complex with plasmid DNA. Hum Gene Ther. 1999;10:2657–65.
8. Choi YH, Liu F, Kim JS, Choi YK, Park JS, Kim SW. Polyethylene glycol-grafted poly-lysine as polymeric gene carrier. J Control Release. 1998;54:39–48.
9. Vinogradov SV, Bronich TK, Kabanov AV. Self-assembly of polyamine-poly(ethylene glycol) copolymers with phosphorothioate oligonucleotides. Bioconjug Chem. 1998;9:805–12.
10. Kakizawa Y, Kataoka K. Block copolymer micelles for delivery of gene and related compounds. Adv Drug Deliv Rev. 2002;54:203–22.
11. Chang SF, Chang HY, Tong YC, Chen SH, Hsaio FC, Lu SC, Liaw J. Nonionic polymeric micelles for oral gene delivery in vivo. Hum Gene Ther. 2004;15:481–93.
12. Katayose S, Kataoka K. Water-soluble polyion complex associates of DNA and poly(ethylene glycol)–poly(L-lysine) block copolymer. Bioconjug Chem. 1997;8:702–7.
13. Katayose S, Kataoka K. Remarkable increase in nuclease resistance of plasmid DNA through supramolecular assembly with poly(ethylene glycol)-poly(L-lysine) block copolymer. J Pharm Sci. 1998;87:160–3.
14. Pasternack RF, Bustamante C, Collings PJ, Giannetto A, Gibbs EJ. Porphyrin assemblies on DNA as studied by a resonance light scattering technique. J Am Chem Soc. 1993;115:5393–9.
15. Huang CZ, Li YF. Resonance light scattering technique used for biochemical and pharmaceutical analysis. Anal Chim Acta. 2003;500:105–17.
16. Li YF, Huang CZ, Huang XH, Li M. Determination of proteins based on their resonance light scattering enhancement effect on Alcian Blue 8GX. Anal Sci. 2000;16:1249–54.
17. Liu RT, Yang JH, Wu X, Sun CX. Interaction of cetyltrimethylammonium bromide with nucleic acids and determination of nucleic acids at nanogram levels based on the measurement of light scattering. Anal Chim Acta. 2001;441:303–8.
18. Li ZP, Li KA, Tong SY. Determination of nucleic acids in acidic medium by enhanced light scattering of large particles. Talanta. 2000;51:63–70.
19. Zhou YL, Li YZ. The interaction of poly(ethylenimine) with nucleic acids and its use in determination of nucleic acids based on light scattering. Spectrochim Acta Part A. 2004;60:377–84.
20. Zhou YL, Li YZ. Determination of the concentration of nucleic acids based on light scattering of a complex formed with poly(allylamine hydrochloride). Anal Lett. 2003;36:2835–47.
21. Wang M, Yang JH, Wu X, Huang F. Study of the interaction of nucleic acids with acridine red and CTMAB by a resonance light scattering technique and determination of nucleic acids at nanogram levels. Anal Chim Acta. 2000;422:151–8.
22. Zeng YB, Cai LL, Wang HD, Li L, You WJ, Guo LH, Chen GN. Resonance light scattering study on the interaction between quinidine sulfate and congo red and its analytical application. Luminescence. 2010;25:30–5.
23. Liu RT, Yang JH, Sun CX, Wu X, Li L, Su BY. Study on the interaction between nucleic acids and cationic surfactants. Colloids Surf B Biointerfaces. 2004;34:59–63.
24. Li L, Xu ZS, Pan Q, Song GW. Determination of nucleic acid based on increased resonance light-scattering of fluorinated surfactants. J Fluor Chem. 2009;130:567–72.
25. Yang CX, Li YF, Feng P, Huang CZ. Study on the interaction of aluminum ion with deoxyribonucleic acid by resonance light scattering measurement. Chin J Anal Chem. 2002;30:473–7.
26. Hao YM, Shen HX. Simple and sensitive determination of nucleic acids using palladium(II) complex with 2-(2-thiazolylazo)-5-dimethylaminobenzoic acid. Anal Chim Acta. 2000;422:159–66.
27. Li J, Kang J, Lu J, Li XZ, Tang JL, Zhang HQ, Zhang YH. Determination of calf thymus DNA using resonance light-scattering quenching method based on the terbium (Tb^{3+})/europium (Eu^{3+})–quercetin system. J Luminesc. 2009;129:906–11.
28. Zhou F, Yang ZG, Zhai C, Ma LX, Chen SY. Complexes micells of block copolymer PLL–PEG–PLL/DNA. Chem Bioeng. 2004;5:26–8.
29. Reschel T, Konák C, Oupický D, Seymour LW, Ulbrich K. Physical properties and in vitro transfection efficiency of gene delivery vectors based on complexes of DNA with synthetic polycations. J Control Release. 2002;81:201–17.
30. Petrov AI, Khalil DN, Kazaryan RL, Savintsev IV, Sukhorukov BI. Structural and thermo-dynamic features of complexes formed by DNA and synthetic polynucleotides with dodecylamine and dodecyltrimethylammonium bromide. Bioelectrochemistry. 2002;58:75–85.
31. Thomas TJ, Messner RP. Structural specificity of polyamines in left-handed Z-DNA formation: immunological and spectroscopic studies. J Mol Biol. 1988;201:463–7.

32. He Y, Song GW, Zou QC. Spectra analysis of interaction between poly((2-methylacryloxyethyl) dimethyl buthylammonium bromide) and nucleic acids. Sens Actuators B. 2005;106:325–30.
33. Winnik FM, Regismond SA, Goddard ED. Interactions of an anionic surfactant with a fluorescent-dye-labeled hydrophobically-modified cationic cellulose ether. Langmuir. 1997;13:111–4.
34. Pi YY, Shang YZ, Liu HL, Hu Y, Jiang JW. Salt effect on the interactions between Gemini surfactant and oppositely charged polyelectrolyte in aqueous solution. J Colloid Interface Sci. 2007;306:405–10.
35. Fundin J, Hansson P, Brown W, Lidegran I. Poly(acrylic acid)-cetyltrimethylammonium bromide interactions studied using dynamic and static scattering and time-resolved fluorescence quenching. Macromolecules. 1997;30:1118–26.